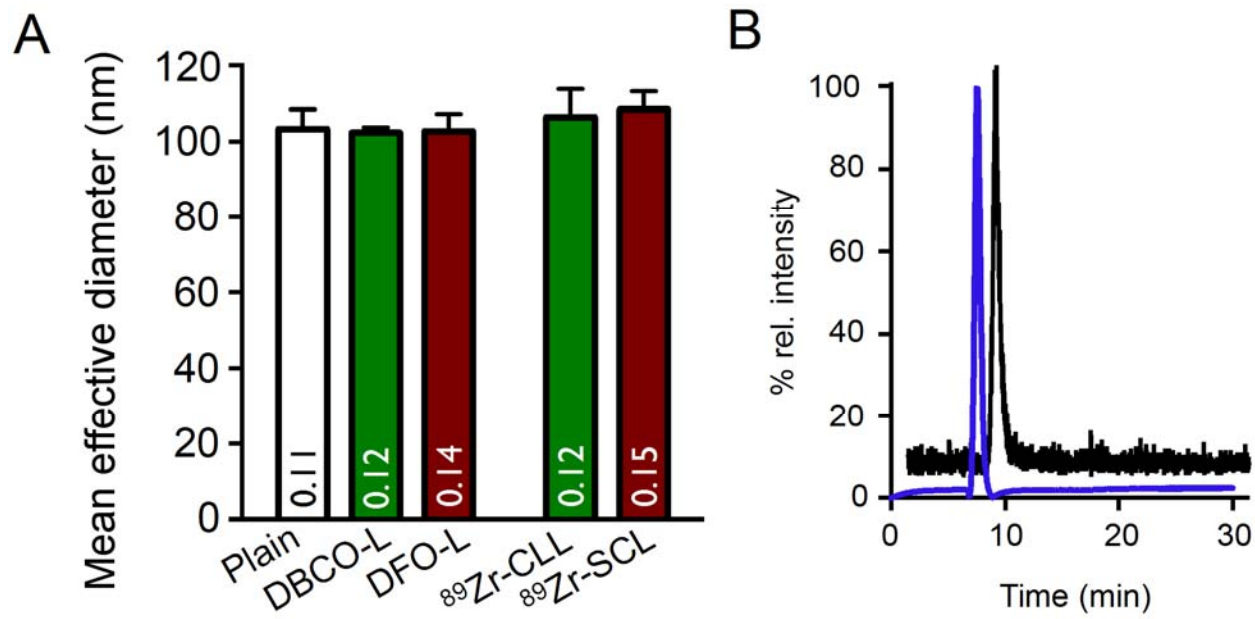
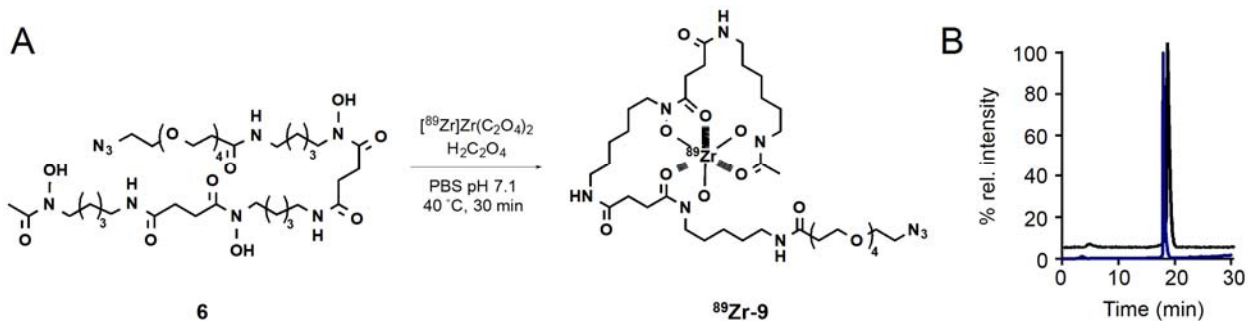


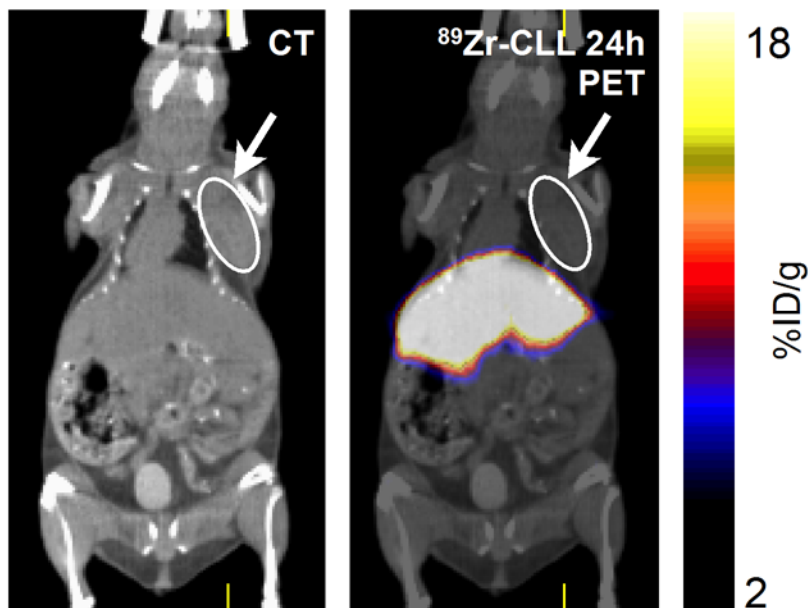
**Supplemental Figure 1.** Synthesis of building blocks **3**, **6**, and **8**, and corresponding mass spectra.



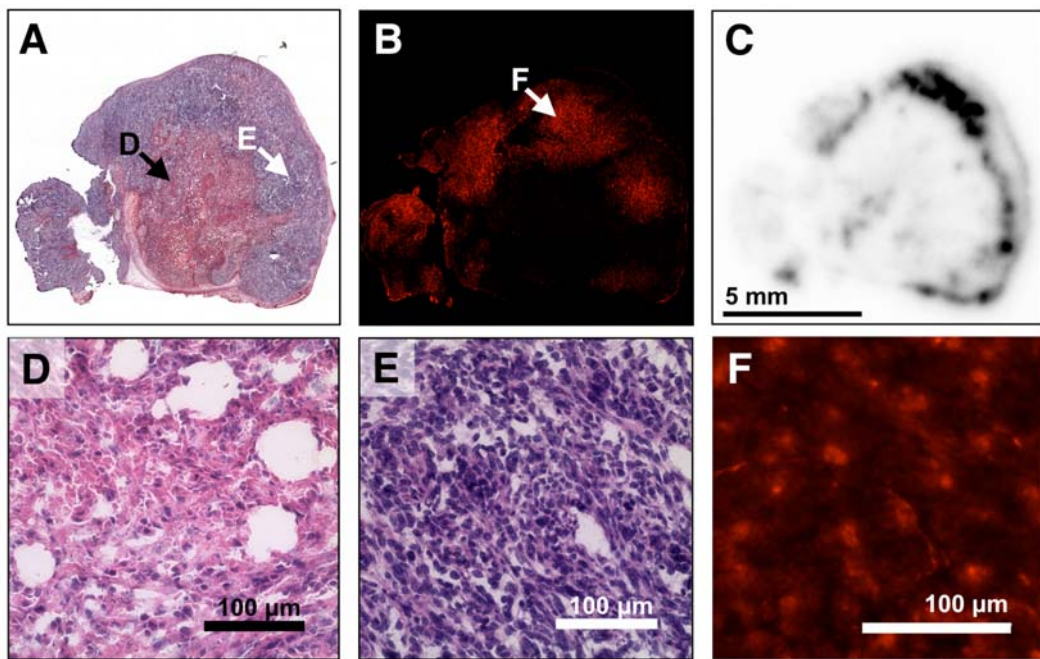
**Supplemental Figure 2.** (A) Sizes (expressed as mean effective diameter) and polydispersity values of different liposomes described in the present work. (B) Size-exclusion chromatogram showing absorption at 650 nm (front) and radioactive trace (back) of sample of DiIC@<sup>89</sup>Zr-SCL.



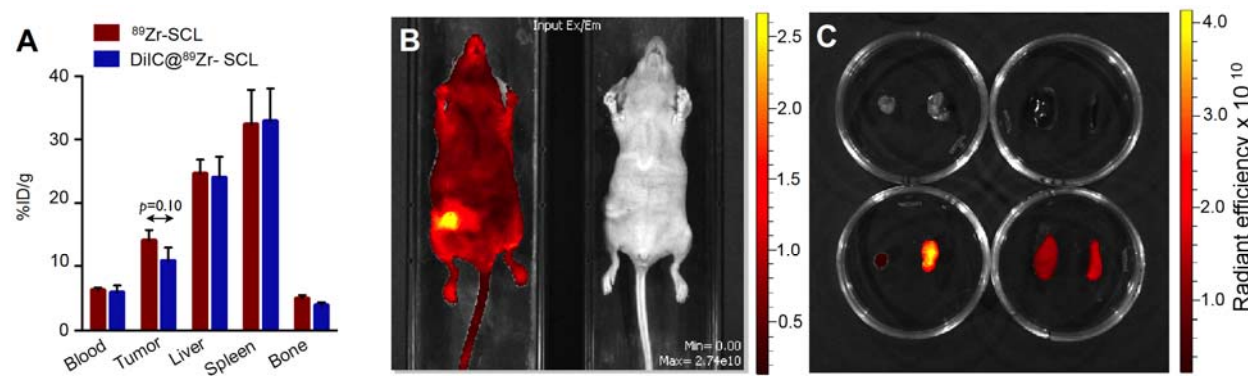
**Supplemental Figure 3.** (A) Radiosynthesis of  $^{89}\text{Zr}$ -9. (B) HPLC chromatogram showing ultraviolet (absorption at 220 nm, front) and radioactive (back) traces of mixture of  $^{89}\text{Zr}$ -9 and reference compound 9, demonstrating coelution.



**Supplemental Figure 4.** PET/CT imaging of  $^{89}\text{Zr}$ -CLL showing CT only (left) and PET/CT fusion (right) at 24 h after injection. Arrow indicates location of tumor.



**Supplemental Figure 5.** Ex vivo analysis of tumor section at 24 h after administration of  $^{89}\text{Zr}$ -SCL. (A) Hematoxylin and eosin staining (expanded regions shown in D and E). (B) IBA1 immunohistology section (expanded region shown in F). (C) Autoradiography.



**Supplemental Figure 6.** (A) PET-quantified radioactivity distribution in selected tissues 24 h after administration of  $^{89}\text{Zr}$ -SCL (left) and DiIC@ $^{89}\text{Zr}$ -SCL (right), expressed as %ID/g  $\pm$  SD ( $n \geq 3$ ). (B) Whole-body near-infrared fluorescence imaging ( $\lambda_{\text{Ex}} = 650 \text{ nm}/\lambda_{\text{Em}} = 670 \text{ nm}$ ) at 24 h after administration of DiIC@ $^{89}\text{Zr}$ -SCL (left) and  $^{89}\text{Zr}$ -SCL (right), which was used as control. (C) Near-infrared fluorescence imaging ( $\lambda_{\text{Ex}} = 650 \text{ nm}/\lambda_{\text{Em}} = 670 \text{ nm}$ ) of excised specimens of muscle, tumor, liver, and spleen (from left to right) collected at 24 h after administration of  $^{89}\text{Zr}$ -SCL (top 2 dishes) and DiIC@ $^{89}\text{Zr}$ -SCL (bottom 2 dishes).

**SUPPLEMENTAL TABLE 1.** Tissue Radioactivity Distribution of  $^{89}\text{Zr}$ -SCL in Female NCr Nude Mice Bearing 4T1 Breast Xenografts ( $n \geq 3$  for Each Time Point)

Tissue	2 h		24 h		48 h	
	%ID/g	SD	%ID/g	SD	%ID/g	SD
<b>Blood</b>	36.9	1.65	6.81	0.29	1.89	0.76
<b>Tumor</b>	3.29	1.11	13.7	1.84	7.88	1.16
<b>Heart</b>	0.97	0.19	1.14	0.14	1.26	0.07
<b>Lungs</b>	1.12	0.35	1.05	0.22	1.03	0.15
<b>Stomach</b>	1.30	0.51	1.57	0.39	0.76	0.07
<b>Small intestine</b>	2.62	1.07	2.72	0.49	1.41	0.10
<b>Large intestine</b>	1.95	0.97	1.56	0.23	0.93	0.05
<b>Spleen</b>	33.5	4.72	58.9	12.2	36.0	7.03
<b>Kidneys</b>	2.64	0.50	3.36	0.43	3.19	0.21
<b>Liver</b>	17.1	6.22	24.7	4.59	22.2	6.15
<b>Muscle</b>	0.85	0.01	1.13	0.09	1.77	0.78
<b>Bone</b>	1.50	0.32	3.78	0.08	5.09	1.32

**SUPPLEMENTAL TABLE 2.** Tissue Radioactivity Distribution of  $^{89}\text{Zr}$ -CLL in Female NCr Nude Mice Bearing 4T1 Breast Xenografts ( $n \geq 3$  for Each Time Point)

Tissue	2 h		24 h		48 h	
	%ID/g	SD	%ID/g	SD	%ID/g	SD
<b>Blood</b>	5.53	0.35	1.04	0.20	0.68	0.24
<b>Tumor</b>	1.23	0.26	2.00	0.15	1.73	0.19
<b>Heart</b>	0.80	0.06	0.82	0.23	0.67	0.26
<b>Lungs</b>	1.19	0.06	0.72	0.16	0.71	0.28
<b>Stomach</b>	0.59	0.15	0.42	0.05	0.40	0.10
<b>Small intestine</b>	0.51	0.09	0.27	0.04	0.28	0.05
<b>Large intestine</b>	0.52	0.12	0.27	0.03	0.22	0.10
<b>Spleen</b>	54.3	14.3	51.4	6.14	23.3	7.29
<b>Kidneys</b>	2.40	0.65	2.75	0.17	3.24	0.40
<b>Liver</b>	49.7	13.0	46.7	5.49	40.1	8.34
<b>Muscle</b>	1.42	0.24	1.19	0.35	0.99	0.47
<b>Bone</b>	2.59	0.92	5.53	1.57	6.16	1.83